DOI: 10.48011/asba.v2i1.1239

Effects of Wave Propagation Velocity on Fault Location Approaches in Power Distribution Systems

Leonardo R. Fernandes
Department of Systems and Energy
University of Campinas
Campinas-SP, Brazil
l190754@dsee.fee.unicamp.br

Victor P. Dardengo
LEPAC
Federal University of Espirito Santo
victor.dardengo@ufes.br

Thiago R. Fernandes
Department of Systems and Energy
University of Campinas
Campinas-SP, Brazil
l190754@dsee.fee.unicamp.br

***Abstract*—To reduce the frequency and duration of interruptions on the energy supply, electric utilities should adopt efficient fault location approaches. Traveling wave-based methods are a good alternative for fault location, as they are more accurate, faster, and less affected by the fault characteristics than the traditional impedance-based approaches. Basically, the accuracy of traveling wave-based approaches depends on the precise identification of the wavefronts arrival times in the meters, as well as on their traveling wave velocities. However, most of the traveling wave-based approaches adopt a single traveling wave velocity to estimate fault locations, which may affect the accuracy of the estimates since the waves tend to travel at different velocities in conductors with different physical characteristics. This paper investigates the effects of wave propagation velocities on fault location estimates via traveling wave-based approaches. Mathematical morphology is used to identify the arrival time of the traveling waves generated by faults on the meters. Different velocities, calculated based on the electrical parameters of the network conductors, are used to determine the fault location in a real distribution system.**

***Index Terms*—Fault location, wave propagation velocity, traveling waves, mathematical morphology, distribution systems.**

I. INTRODUCTION

The industrial development and population growth have caused an increase in complexity and size of distribution systems, which provided the emergence of new regulatory standards, requiring higher reliability, security, and quality of power supplies [1], [2], [3], [4]. Due to equipment failure, traffic accidents, animals, trees, weather conditions, etc., the incidence of short-circuits in the network is the major cause of interruptions on the energy supply system.

To reduce the frequency and duration of interruptions on the energy supply, and decrease the economic and social losses, effective fault location approaches should be adopted by electric utilities [5]. The most used fault location approaches in distribution systems are impedance- and traveling wave-based methods [1], [6], [7], [8]. Impedance-based approaches use voltages, currents, and network parameters information to estimate the distance from a meter to the fault incidence location. In some cases, load parameters are also needed.

Traveling wave approaches are more accurate, faster, and less affected by the fault resistance, fault inception angle, and fault type than the impedance-based approaches [9]. However, these approaches require equipment with high sampling rates and algorithms capable of identifying the instant of arrival of the wavefronts to the meters. Consequently, they are more complex, costly, and may require time synchronization [10]. Traveling wave approaches use the information contained in the transients of current and voltage signals generated by the faults. Then, the fault location is estimated through the wavefronts' arrival time on the meters and the velocity of the traveling wave specified. These approaches can be based on one- or two-terminal methods [6].

The accuracy of traveling wave approaches by one- or two-terminal methods depends, among other factors, on the precise identification of the wavefronts arrival times in the meters, as well as on their traveling wave velocities. Several approaches have been proposed in the literature to identify the wavefronts and detect their arrival times, among which Wavelet Transform (WT) [11], and Mathematical Morphology (MM) [12] can be highlighted. Although WT is traditionally more used, due to easy implementation and low computational costs, MM emerges as a good alternative. Unlike WT, which operates in time and frequency domains, MM acts on signal waveforms directly in the time domain. It combines basic morphological operations formed by addition, subtraction, maximum and minimal operations, modifying or preserving the desired information of the signals [12].

Traveling wave velocities are calculated using electrical parameters such as the positive-sequence series impedance and shunt admittance of the network. In typical distribution systems, the network conductors have different physical characteristics, implying distinct electrical parameters. Moreover, these parameters change over the years due to the aging of the conductors. Therefore, adopting a single traveling wave velocity to estimate fault locations via traveling wave approaches may affect the accuracy of the estimates [13]. As such, it is crucial to understand the effects of wave propagation velocities on fault location estimates in distribution systems.

In this context, this paper analyzes the effects of the wave velocities on two-terminal traveling waves-based fault location methods that use only a single velocity to estimate fault location in distribution systems. To this end, faults are applied in a real distribution feeder modeled in ATP/EMPT, with several available meters, and the fault locations are calculated for each pair of meters using different traveling wave velocities.

Clarke's modal transformation is used to decouple the signals in the phase domain into modal components. MM is applied as a digital signal processing technique to detect the arrival times of traveling waves in the meters from the signals in the modal form.

The remainder of the paper is organized as follows. In Section II, the basic concepts of traveling waves fault location theory, and the two-terminal method is presented. Section III reviews the basic concepts of MM and Clarke's modal transformation. Case studies are presented in Section IV. Finally, conclusions are drawn in Section V.

II. traveling Waves Based Fault Location Approaches Concepts

When a fault occurs in a power system, traveling waves originate in the voltage and current signals. These waves travel from the fault point F towards the line terminals, suffering reflections, refractions, and attenuation. Fig. 1 presents a Bewley's lattice diagram, where the continuous and dashed lines represent, respectively, reflections and refractions [6], [12].

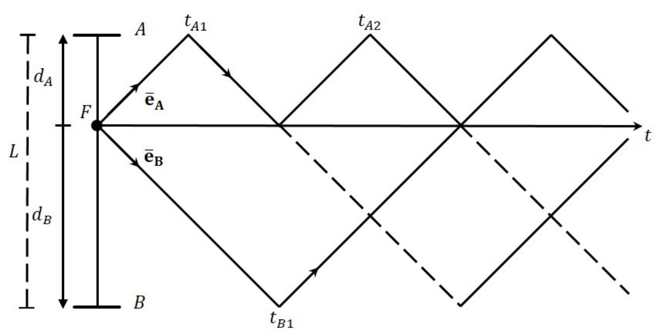

Fig. 1. Bewley's lattice diagram. [6]

From Bewley's lattice diagram shown in Fig. 1, the distance from the fault to terminal A (d_A) can be calculated by (1) or (2) using data from one or two meters, where t_{A1} and t_{B1}, and t_{A2}, respectively, the arrival times of the first and second wavefronts reaching the terminals A and B, v is the wave velocity, and L is the transmission line length. [6], [14].

$$d_A = \frac{(t_{A2} - t_{A1}) \cdot v}{2} \tag{1}$$

$$d_A = \frac{L + (t_{A1} - t_{B1}) \cdot v}{2} \tag{2}$$

In this paper, the two-terminal approach is used to estimate the fault location. Morphological filters are used to identify the arrival times of traveling waves in the monitored terminals. The wave velocity v is calculated based on the line parameters, as shown in (3), where L_1 and C_1 are, respectively, the positive-sequence inductance, and shunt capacitance.

$$v = \frac{1}{\sqrt{L_1 C_1}} \tag{3}$$

In typical distribution systems, the network conductors have more than one electrical parameter configuration. According to the meter positions, the traveling waves can travel through the network conductors with different parameters at different velocities. Therefore, defining the correct traveling wave velocity needed to estimate the fault location distance from the meter is a challenging task.

III. Mathematical Morphology and Clarke's Transformation

To highlight the wavefronts and identify its arrival times on the meters, MM is used. In MM, two basics operators, the so-called dilation, and erosion, operate directly in the time domain, modifying the geometric aspect of the signal locally [15], [12], [16]. These operators are calculated using addition, subtraction, and extraction of maxima and minima, representing a practical and computationally efficient tool.

Dilation and erosion are defined, respectively, by (4) and (5), where $f(z)$ is the input signal, and $g(s)$ the Structuring Element (SE), defined in the domains $D_f = \{0, 1, ..., z-1\}$ and $D_g = \{0, 1, ..., s-1\}$, with $z > s$, where z and s are integers.

$$(f \oplus g)(z) = max \begin{Bmatrix} f(z-s) + g(s), \\ 0 \le (z-s) \le z, s \ge 0 \end{Bmatrix} \tag{4}$$

$$(f \ominus g)(z) = min \begin{Bmatrix} f(z+s) - g(s), \\ 0 \le (z-s) \le z, s \ge 0 \end{Bmatrix} \tag{5}$$

Depending on the morphological filter type and SE, different characteristics of the signal can be highlighted or attenuated. In this paper, the Multi-Resolution Morphological Gradient (MMG) is used to highlight the wavefronts reaching the monitored terminals.

A. Multi-Resolution Morphological Gradient

MMG aims to depress stationary components and highlight transients, extracting the rising and falling edges though two flat SEs with opposite origins, as shown in (6) and (7), in which the underlined element represents the origin of the SE with size l [12]. In a flat SE, all elements are equal.

$$g^{+} = \{0_1, 0_2, ..., \underline{0_l}\} \tag{6}$$

$$g^{-} = \{\underline{0_1}, 0_2, ..., 0_l\} \tag{7}$$

The MMG is defined by (8), where $\rho^a_{g^+}$ and $\rho^a_{g^-}$ are given, respectively, by (9) and (10). The resolution level of the MMG is indicated by a [12].

$$\rho^{a}{}_{g} = \rho^{a}{}_{g^+} + \rho^{a}{}_{g^-} \tag{8}$$

$$\rho^{a}{}_{g^+} = (\rho^{(a-1)} \oplus g^+)(x) - (\rho^{(a-1)} \ominus g^+)(x) \tag{9}$$

$$\rho^{a}{}_{g^-} = (\rho^{(a-1)} \ominus g^-)(x) - (\rho^{(a-1)} \oplus g^-)(x) \tag{10}$$

B. Clarke's Modal Transformation

The voltage signals in phase domain are decoupled into modal components through Clarke's modal transformation to eliminate the influence that the phases wave propagation velocities have on each other and identify the arrival times wavefronts reach the meters. Clarke's modal transformation is defined by (11), where $\overline{V}_a$, $\overline{V}_b$ and $\overline{V}_c$ represent the phase domain of the voltage signal and $\overline{V}_\alpha$, $\overline{V}_\beta$ and $\overline{V}_0$ are the voltage signal decoupled into modal components [17].

$$\begin{bmatrix} \overline{V}_\alpha \\ \overline{V}_\beta \\ \overline{V}_0 \end{bmatrix} = \begin{bmatrix} \frac{2}{\sqrt{6}} & \frac{-1}{\sqrt{6}} & \frac{-1}{\sqrt{6}} \\ 0 & \frac{1}{\sqrt{2}} & \frac{-1}{\sqrt{2}} \\ \frac{1}{\sqrt{3}} & \frac{1}{\sqrt{3}} & \frac{1}{\sqrt{3}} \end{bmatrix} \cdot \begin{bmatrix} \overline{V}_a \\ \overline{V}_b \\ \overline{V}_c \end{bmatrix} \tag{11}$$

IV. Case Studies

Since by (2) only a single traveling wave velocity can be adopted to calculate the fault location, the selection of the traveling wave velocity can be a significant source of errors in the fault location estimates.

To evaluate the impact of the velocity of the traveling waves in fault location estimation, estimates using two distinct velocities are computed. Simulations are performed on the real 21-bus, 25 kV *SaskPower* distribution network [18] (Fig. 2), modeled in the ATP-EMPT [19]. Single-phase-to-ground (SPG) faults are performed, as this is the most common type of fault in distribution systems [4].

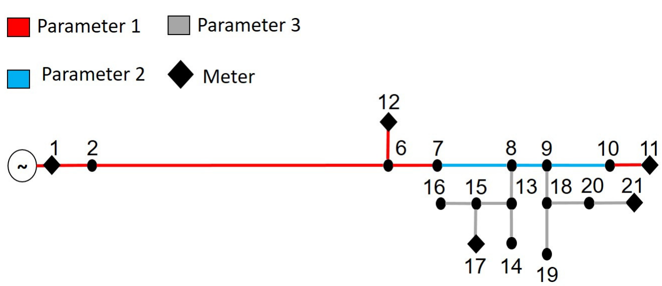

Fig. 2. *SaskPower* Network

The velocities are the [20]:

(i) Arithmetic Mean Velocity (AMV), which corresponds to the arithmetic mean of the wave propagation velocities in the electrical parameters between the meters, given by (12), where r is the amount of electrical parameter configurations between the meters.

(ii) Weighted Arithmetic Mean Velocity (WAMV), which corresponds to the arithmetic mean considering the length of each branch contained between each pair of meters, given by (13), where v_{wamv} is the WAMV velocity, n is the number of branches between the meters, w is the branch length against the distance between the meters, and $v_{(k-m)_i}$ is the propagation velocity of the waves associated with the electrical parameters of each branch connected by buses k and m.

$$v_{amv} = \frac{v(1) + v(2) + \ldots + v(r)}{r} \tag{12}$$

$$v_{wamv} = \frac{\sum_{i=1}^{n} w_i \cdot v_{(k-m)_i}}{\sum_{i=1}^{n} w_i} \tag{13}$$

If there are different types of electrical parameters between two meters, first, the velocities associated with each type are calculated by (3). Then the AMV and WAMV velocities of the pairs of meters are computed.

Due to the insensitivity of traveling-waves-based methods to fault resistance value and type [6], a single fault resistance of 1 Ω is considered for the simulations. The sample rate used is 1.2 MHz, and meters are allocated on buses 1, 11, 12, 17, and 21. SLG faults (on phase A) are performed at buses 2, 6, 7, 8, 9, 10, 13, 15, 18, and 20. The pairs of meters 1-11, 1-12, 1-17, 1-21, and 17-21 are chosen to evaluate the presence of one, two, and three velocities.

The positive-sequence impedance and shunt capacitance, as well as the propagation velocities, are shown in Table I. For more information about the network, refer to [18]. The distance between each pair of meters, WAMV and AMV propagation velocities, as well as the branch lengths, are summarized in Tables II, and III, respectively. Once the fault locations are estimated, the errors are given by (14), where d_{est} and d_{actual} are, respectively, the estimated and actual distances from the bus with metering to the fault location. The actual distances from the buses with meters to the fault location, considering the pairs of meters defined previously, are summarized in Table IV.

$$error = |d_{est} - d_{actual}| \tag{14}$$

TABLE I
POSITIVE-SEQUENCE ELECTRICAL PARAMETERS - *SaskPower* [18]

-	Electrical Parameters		
	1	2	3
Series impedance (Ω/km)	0.3480 + j0.5166	0.5519+ j0.5390	7.3977 + j0.8998
Shunt admittance Mhos/km	j3.74$\times 10^{-6}$	j3.59$\times 10^{-6}$	j2.51$\times 10^{-6}$
Propagation velocity (km/s)	271.21 $\times 10^3$	271.01 $\times 10^3$	250.85 $\times 10^3$

A. Discussion

It is important to highlight that, for faults occurring outside the path between the meters, the traveling wave-based methods point to the closest bus as the fault location [4]. For this reason, only the buses between the meters of each pair of meters are tested. Assuming that the faults have already been detected, the results are presented as follows.

TABLE II
WAMV AND AMV VELOCITIES AND DISTANCES BETWEEN METERS

Pair of meters	Dist. between meters (km)	AMV (km/s)	WAMV (km/s)
1-11	37.01	271.11×10^3	271.15×10^3
1-12	20.92	271.21×10^3	271.21×10^3
1-17	34.92	264.36×10^3	266.96×10^3
1-21	38.94	264.36×10^3	266.54×10^3
17-21	18.50	260.93×10^3	253.48×10^3

TABLE III
BRANCHES LENGTHS

Branch	Length (km)
1-2; 8-9; 10-11; 11-12; 8-13; 13-14; 13-15; 15-16; 15-17; 9-18; 18-19	2.414
2-6	16.092
6-7	4.023
7-8	5.150
9-10	4.506
18-20; 20-21	3.219

TABLE IV
ACTUAL FAULT LOCATION

Fault distance (km)			
Faulted bus	Bus with meter		
	1	11	17
2	2.41	-	-
6	18.50	-	-
7	22.52	-	-
8	27.67	9.33	7.24
9	30.09	6.92	9.65
10	34.59	2.41	-
13	30.09	11.74	4.82
15	32.50	14.16	2.41
18	32.50	-	12.07
20	35.72	-	15.28

The errors obtained from estimating the fault locations using the AMV are shown in Table V, whereas the errors of the estimates calculated using the WAMV are presented in Table VI. Analyzing the results shown in tables V and VI, it is observed that the estimates found by the pair of meters 1-12 are equal. This is due to the presence of a single electrical parameter between the meters at buses 1 and 12, resulting in equal AMV and WAMV. The estimates present good accuracy, as a single propagation velocity does not represent a significant source of errors.

The pairs of meters 1-11 and 17-21 have two electrical parameters associated with them. The pair 1-11 has the Parameters 1 and 2, which have propagation velocities much alike (see Table I). Therefore, their AMV and WAMV presented almost the same values (271.12×10^3 and 271.15×10^3 km/s, respectively), resulting in estimate errors slightly different. On the other hand, the pair 17-21, despite similar estimation errors, have parameter configurations (2 and 3) with propagation velocities much different (see Table I). Such estimates were achieved as a result of the similar values of AMV and WAMV (260.934×10^3 and 253.483×10^3 km/s, respectively), obtained as a result of the predominance of the Parameter 3 between the meters 17 and 21.

Concerning the pairs of meters 1-17 and 1-21, which have three electrical parameters between their meters, it is observed that, in most cases, using the WAMV slightly enhances the estimation accuracy. This is due to the contribution of each electrical parameter to this propagation velocity. For example, considering a fault at bus 2, the waves traveling through the branches cover a distance significantly shorter through Parameter 3 than through Parameters 1 and 2, implying a WAMV velocity slightly greater than the AMV (see Table II). Figs. 3 and 4 illustrate the results shown in tables V, and VI, respectively.

TABLE V
FAULT LOCATION ESTIMATION ERRORS - AMV VELOCITY

Errors (m)					
-	Pair of meters				
Faulted bus	1-11	1-12	1-17	1-21	17-21
2	61	22.7	66.6	96	-
6	112	22.7	384.4	355	-
7	69	-	442.5	413	-
8	23	-	525.6	606.4	53.6
9	48	-	-	597.2	76
10	61	-	-	-	-
13	-	-	406.2	-	31.6
15	-	-	287	-	226.6
18	-	-	-	477.8	11
20	-	-	-	282.1	162

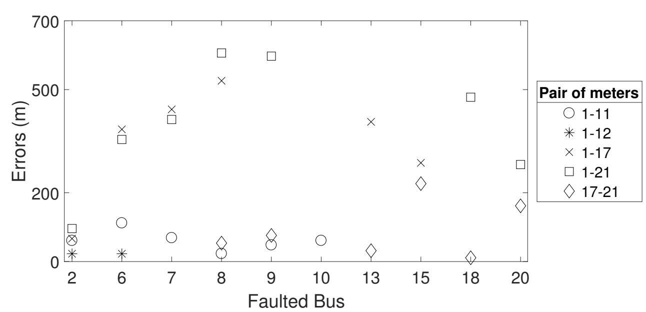

Fig. 3. Fault location estimation errors - AMV velocity

TABLE VI
FAULT LOCATION ESTIMATION ERRORS - WAMV VELOCITY

Errors (m)					
-	Pair of meters				
Faulted bus	1-11	1-12	1-17	1-21	17-21
2	63	22.7	80.9	44.5	-
6	112.4	22.7	377.9	366	-
7	68.4	-	397	391	-
8	21.6	-	430.2	543.5	5.4
9	49.8	-	-	514.3	85.2
10	63	-	-	-	-
13	-	-	285.8	-	95.7
15	-	-	141.6	-	24.8
18	-	-	-	373.8	70
20	-	-	-	150	15

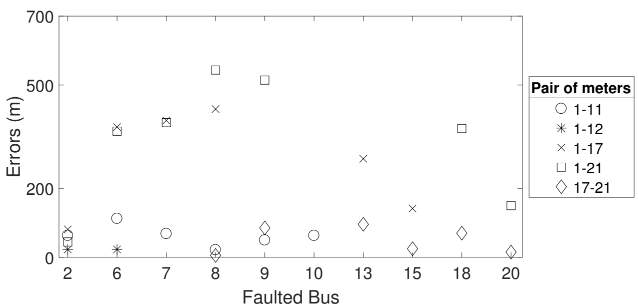

Fig. 4. Fault location estimation errors - WAMV velocity

V. CONCLUSION

This paper discusses how the use of a single propagation velocity affects the accuracy of fault detection algorithms based on traveling wave approaches. Through the analysis of fault simulations in a real distribution system, it is shown that the velocity plays an important role in fault detection in situations where there is more than one electrical parameter associated with the conductors of the network.

For faults occurring on a path between two meters where there are similar electrical parameters with close wave propagation velocities associated with them, the obtained estimates were close and presented good accuracy, reaching estimate errors of around 20 m. On the other hand, when these velocities were considerably different, the accuracy was compromised. Furthermore, although some results were precise, many other presented errors above 200 m. Estimates using the Weighted Arithmetic Mean Velocity showed better accuracy in most cases. This was achieved as a result of the weighted arithmetic mean of the velocities associated with each electrical parameter configuration, relating the length and electrical parameters of each branch between these meters. The results also showed that determining a single velocity is not a simple task; thus, more studies are needed.

REFERENCES

[1] I. Džafić, R. A. Jabr, S. Henselmeyer, and T. onlagić, "Fault location in distribution networks through graph marking," IEEE Transactions on Smart Grid, vol. 9, no. 2, pp. 1345–1353, March 2018.

[2] K. Sun, Q. Chen, Z. Gao, D. Liu, and G. Zhang, "Generalized impedance-based fault distance calculation mehtod for power distribution systems," in 2014 IEEE PES Asia-Pacific Power and Energy Engineering Conference (APPEEC), Dec 2014, pp. 1–4.

[3] S. F. Alwash, V. K. Ramachandaramurthy, and N. Mithulananthan, "Fault-location scheme for power distribution system with distributed generation," IEEE Transactions on Power Delivery, vol. 30, no. 3, pp. 1187–1195, 2015.

[4] P. A. H. Cavalcante et al., "Técnicas para localização de defeitos em sistemas modernos de distribuição de energia elétrica," 2016.

[5] J. Zhao, T. He, C. Liu, and K. Li, "Travelling wave fault location for distribution line based on improved morphological gradient algorithm," in 2016 International Symposium on Computer, Consumer and Control (IS3C), July 2016, pp. 156–159.

[6] M. M. Saha, J. J. Izykowski, and E. Rosolowski, Fault location on power networks. Springer Science & Business Media, 2010.

[7] K. Jia, Z. Ren, T. Bi, and Q. Yang, "Ground fault location using the low-voltage-side recorded data in distribution systems," IEEE Transactions on Industry Applications, vol. 51, no. 6, pp. 4994–5001, Nov 2015.

[8] J. Coser et al., "Contribuições aos métodos para localização de faltas em alimentadores de distribuição," 2006.

[9] Z. Bo, A. Johns, and R. Aggarwal, "A novel fault locator based on the detection of fault generated high frequency transients," 1997.

[10] R. Liang, G. Fu, X. Zhu, and X. Xue, "Fault location based on single terminal travelling wave analysis in radial distribution network," International Journal of Electrical Power & Energy Systems, vol. 66, pp. 160–165, 2015.

[11] I. Daubechies, "The wavelet transform, time-frequency localization and signal analysis," IEEE transactions on information theory, vol. 36, no. 5, pp. 961–1005, 1990.

[12] Q.-H. Wu, Z. Lu, and T. Ji, Protective relaying of power systems using mathematical morphology. Springer Science & Business Media, 2009.

[13] J. Ding, L. Li, Y. Zheng, C. Zhao, H. Chen, and X. Wang, "Distributed travelling-wave-based fault location without time synchronisation and wave velocity error," IET Generation, Transmission & Distribution, vol. 11, no. 8, pp. 2085–2093, 2017.

[14] F. H. Magnago and A. Abur, "Fault location using wavelets," IEEE Transactions on Power Delivery, vol. 13, no. 4, pp. 1475–1480, 1998.

[15] S. Gautam and S. M. Brahma, "Overview of mathematical morphology in power systems—a tutorial approach," in Power & Energy Society General Meeting, 2009. PES'09. IEEE. IEEE, 2009, pp. 1–7.

[16] E. R. Dougherty and R. A. Lotufo, Hands-on morphological image processing. SPIE press, 2003, vol. 59.

[17] E. Clarke, Circuit analysis of AC power systems. Wiley, 1943, vol. 1.

[18] R. Das, Determining the locations of faults in distribution systems, 1998.

[19] ATP-EMTP. (1994) ATP-EMTP software description, downloads and forums. [Online]. Available: https://www.emtp.org

[20] A. Leon-Garcia, "Probability, statistics, and random processes for electrical engineering," 2017.